

Evaluation of effective thermoelastic properties of random fibrous composites

M. Šejnoha

Assistant Professor

Czech Technical University in Prague

Faculty of Civil Engineering

Department of Structural Mechanics

Thákurova 7

166 29, Prague 6

sejnom@fsv.cvut.cz

J. Zeman

Ph.D. student

Czech Technical University in Prague

Klokner Institute

Department of Mechanics

Šolínova 7

166 08, Prague 6

zeman@klok.cvut.cz

J. Šejnoha

Professor

Czech Technical University in Prague

Faculty of Civil Engineering

Department of Structural Mechanics

Thákurova 7

166 29, Prague 6

sejnoha@fsv.cvut.cz

Abstract

Effective thermoelastic material properties are found for random fibrous composite systems. In particular, the graphite fiber tow embedded in the polymer matrix is selected as a representative of the two-phase disordered composite media. Two approaches to the evaluation of effective properties are described. The first one utilizes the extended form of the Hashin-Shtrikman variational principle, which directly incorporates certain microstructure describing functions to generate bounds on effective thermoelastic properties. The second approach relies on construction of a periodic unit cell, which statistically resembles the real microstructure. Standard homogenization procedure based on the stress control is then invoked to generate a system of governing equations for estimation of the overall thermoelastic properties of the composite. Several numerical results are presented for the selected material system.

1 Introduction

The purpose of this paper is to introduce two different approaches to the evaluation of thermoelastic response of composite materials with random microstructure.

Typically, evaluation of local fields in such a medium is limited to application of various approximate techniques such as the self-consistent or Mori-Tanaka methods [4].

However, when a certain knowledge of the real microstructure is available, the estimates of local fields can be improved by treating random composites. To that end, the random character of a real microstructure can be incorporated through various statistical descriptors directly into variational principles, which readily provide bounds on overall elastic properties of heterogeneous media. Usually, the two-point [3] or even three-point [7] probability functions are used to describe microstructure morphology. However, since three-point functions are quite difficult to obtain for real microstructures, the description by two-point probability functions is preferable.

Another treatment is available when considering periodic microstructures. In such a case, the real microstructure, see Fig. 1, is replaced by a material representative volume element given in terms of a periodic unit cell, which statistically resembles the actual composite. The elements of this approach have been outlined in our previous work [12] when estimating overall mechanical properties of a graphite fiber tow impregnated by the polymer matrix.

Section 2 briefly reviews the basic aspects associated with quantification of microstructure morphology. Section 3 introduces the extended form of the well-known Hashin-Shtrikman variational principle and discusses its application for obtaining bounds on the overall thermomechanical properties of the material system under consideration. Section 4 describes the construction of a periodic unit cell and the essence of the numerical method for evaluation of local and overall fields in the periodic media. For the sake of completeness various connections between the local and overall thermal strains are revisited. Example problems are presented in Section 5.

Hereafter, we adopt notation introduced by Beran [1] and denote an ensemble average of a function $\mathbf{u}(\mathbf{x})$ as $\overline{\mathbf{u}(\mathbf{x})}$, while in a volume-averaged sense we write $\langle \mathbf{u}(\mathbf{x}) \rangle$.



Figure 1: A real micrograph of a transverse plane section of the fiber tow

2 Description of a microstructure of random composites

To reflect a random character of heterogeneous media it is convenient to introduce the concept of an *ensemble* - the collection of a large number of systems which are different in their microscopical details, but they are identical in their macroscopic details. Then, effective or expected value of some quantity corresponds to the process of its averaging through all systems, forming the ensemble.

To that end, consider a sample space S with individual members denoted as α . Define $p(\alpha)$ as the probability density of α in S . Then an *ensemble average* of function $F(\mathbf{x}, \alpha)$ at a point \mathbf{x} is provided by

$$\overline{F(\mathbf{x})} = \int_S F(\mathbf{x}, \alpha) p(\alpha) d\alpha. \quad (1)$$

In the context of quantification microstructure morphology, an ensemble represents the collection of material micrographs taken from different samples of the material. To describe a random microstructure we introduce a *characteristic* or *indicator* function $\chi_r(\mathbf{x}, \alpha)$, which is equal to one when point \mathbf{x} lies in phase r in the sample α and equal to zero otherwise

$$\chi_r(\mathbf{x}, \alpha) = \begin{cases} 1 & \mathbf{x} \in D_r(\alpha) \\ 0 & \text{otherwise.} \end{cases} \quad (2)$$

The symbol $D_r(\alpha)$ denotes here the domain occupied by r -th phase in the sample α . For a two-phase fibrous composite, $r = f, m$, characteristic functions $\chi_f(\mathbf{x}, \alpha)$ and $\chi_m(\mathbf{x}, \alpha)$ are related by

$$\chi_m(\mathbf{x}, \alpha) + \chi_f(\mathbf{x}, \alpha) = 1. \quad (3)$$

With the aid of function χ_r , the *general n - point probability function* S_{r_1, \dots, r_n} is given by [1, 10].

$$S_{r_1, \dots, r_n}(\mathbf{x}_1, \dots, \mathbf{x}_n) = \overline{\chi_{r_1}(\mathbf{x}_1, \alpha) \cdots \chi_{r_n}(\mathbf{x}_n, \alpha)}. \quad (4)$$

Thus, S_{r_1, \dots, r_n} gives the probability of finding n points $\mathbf{x}_1, \dots, \mathbf{x}_n$ randomly thrown into a medium located in the phases r_1, \dots, r_n . We limit our attention to functions of the order of one and two.

Analysis of random composites usually relies on various statistical assumptions such as ergodic hypothesis, spatial homogeneity or isotropy, which may simplify the computational effort to a great extent. In particular, the ergodic hypothesis demands all states available to an ensemble of the systems to be available to every member of the system in the ensemble as well [1]. Then, the *spatial* or *volume average* of function $\chi_r(\mathbf{x}, \alpha)$ given by

$$\langle \chi_r(\mathbf{x}, \alpha) \rangle = \lim_{V \rightarrow \infty} \frac{1}{V} \int_V \chi_r(\mathbf{x} + \mathbf{y}, \alpha) d\mathbf{y}, \quad (5)$$

is independent of α and identical to the ensemble average

$$\overline{\chi_r(\mathbf{x})} = \langle \chi_r(\mathbf{x}) \rangle = c_r. \quad (6)$$

For periodic composites represented by a unit cell Ω it assumes the form

$$\lim_{V \rightarrow \infty} \frac{1}{V} \int_V \chi_r(\mathbf{x} + \mathbf{y}, \alpha) d\mathbf{y} = \frac{1}{\Omega} \int_{\Omega} \chi_r(\mathbf{x} + \mathbf{y}, \alpha) d\mathbf{y}. \quad (7)$$

The above assumption is usually accepted as an hypothesis subject to experimental verification. The statistical homogeneity assumption means that the value of the ensemble average is independent of the position of the coordinate system origin. Then, for example, the two-point matrix probability function reads

$$S_{mm}(\mathbf{x}_1, \mathbf{x}_2) = S_{mm}(\mathbf{x}_{12}), \quad (8)$$

where $\mathbf{x}_{ij} = \mathbf{x}_j - \mathbf{x}_i$. When making the statistical isotropy assumption, we assume that the ensemble average is not only independent of the position of the coordinate system origin but of the coordinate system's rotation as well. Then

$$S_{mm}(\mathbf{x}_1, \mathbf{x}_2) = S_{mm}(r_{12}), \quad (9)$$

where $r_{ij} = \|\mathbf{x}_{ij}\|$. For the microstructure in Fig. 1, the validation of ergodic hypothesis and assumption of statistical isotropy is outlined in [12]. When accepting these assumptions, we may exploit a number of other functions, which provide the desired statistics of the composite sample. Here we introduce the pair distribution function g_2

$$g_2(r) = \frac{1}{2\pi r} \frac{dK(r)}{dr}, \quad (10)$$

where K is the second order intensity function [8]. For isotropic and ergodic medium the above descriptors are uniquely related to the two-point matrix probability function S_{mm} [11], in the form

$$\begin{aligned} S_{mm}(r_{12}) &= 1 - \rho V_2(r_{12}) + (\rho \pi R^2)^2 + \rho^2 M(r_{12}) \\ M(r_{12}) &= \iint h(r_{34}) m(r_{13}) m(r_{24}) dr_3 dr_4 \\ h(r) &= g_2(r) - 1 \\ m(r) &= \begin{cases} 1 & r \leq R \\ 0 & \text{otherwise} \end{cases} \\ \rho &= \frac{N}{A}, \end{aligned} \quad (11)$$

where $V_2(r)$ is a union of two circles distant by r and R is the fiber radius. For numerical evaluation of individual functions we refer the reader to [12].

3 Effective properties by Hashin-Shtrikman variational principle

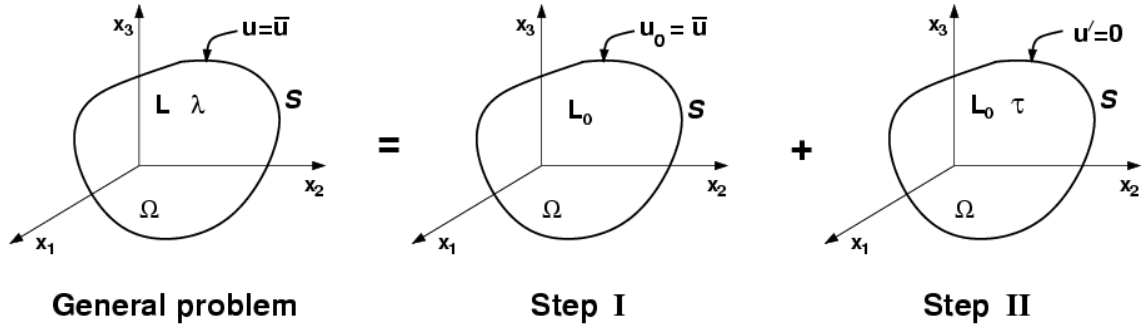


Figure 2: Body with prescribed surface displacements including eigenstresses

This section is devoted to the prediction of the response of random composite materials using the Hashin-Shtrikman variational principle. First, we focus on theoretical aspects associated with the H-S variational formulation for anisotropic and non-homogeneous bodies with displacements $\mathbf{u} = \bar{\mathbf{u}}$ prescribed along the entire boundary S of the composite. In addition, eigenstrains (stress free strains) or eigenstresses are admitted in the present formulation. This formulation then provides rigorous upper and lower bounds on the effective thermoelastic constants of *statistically homogeneous ergodic* composites.

3.1 Body with prescribed surface displacements and eigenstresses

Suppose that an affine displacement field $\mathbf{u}_0(\mathbf{x}) = \mathbf{E}\mathbf{x}$ compatible with a uniform strain \mathbf{E} is prescribed along the boundary S of a homogeneous comparison medium (Step I) characterized by the stiffness matrix \mathbf{L}_0 . The corresponding uniform strain \mathbf{E} and stress $\boldsymbol{\Sigma}$ fields are related through constitutive the law in the form

$$\boldsymbol{\Sigma} = \mathbf{L}_0 \mathbf{E} \quad \text{in } \Omega, \quad \mathbf{u}_0 = \bar{\mathbf{u}} \quad \text{on } S. \quad (12)$$

The local stress $\boldsymbol{\sigma}(\mathbf{x})$ at point \mathbf{x} in Ω of a composite is found by superimposing the solution of the local problem displayed in Fig. 2 Step II. The respective governing equations are then given by

$$\nabla \cdot (\mathbf{L}_0 \boldsymbol{\varepsilon} + \boldsymbol{\tau}) = \mathbf{0} \quad \text{in } \Omega, \quad (13)$$

$$\boldsymbol{\tau} - (\mathbf{L} - \mathbf{L}_0) \boldsymbol{\varepsilon} - \boldsymbol{\lambda} = \mathbf{0} \quad \text{in } \Omega, \quad (14)$$

$$\mathbf{u}' = \mathbf{u} - \mathbf{u}_0 \quad \text{in } \Omega, \quad \mathbf{u}' = \mathbf{0} \quad \text{on } S, \quad (15)$$

$$\boldsymbol{\varepsilon}' = \boldsymbol{\varepsilon} - \mathbf{E} \quad \text{in } \Omega, \quad (16)$$

$$\boldsymbol{\sigma}' = \boldsymbol{\sigma} - \boldsymbol{\Sigma} \quad \text{in } \Omega. \quad (17)$$

The unknown polarization stress $\boldsymbol{\tau}(\mathbf{x})$ is yet to be found such that the local stress derived from the original problem

$$\boldsymbol{\sigma}(\mathbf{x}) = \mathbf{L}(\mathbf{x}) \boldsymbol{\varepsilon}(\mathbf{x}) + \boldsymbol{\lambda}(\mathbf{x}) \quad \text{in } \Omega, \quad \mathbf{u} = \bar{\mathbf{u}} \quad \text{on } S, \quad (18)$$

and the one provided by the two step auxiliary procedure

$$\boldsymbol{\sigma}(\mathbf{x}) = \mathbf{L}_0 \boldsymbol{\varepsilon}(\mathbf{x}) + \boldsymbol{\tau}(\mathbf{x}), \quad (19)$$

are equal. The eigenstress vector $\boldsymbol{\lambda}(\mathbf{x})$ in Eq. (18) may represent several distinct physical phenomena such as thermal effects, shrinkage, plasticity, etc. A formulation equivalent to Eqs. (13) and (14) may be obtained by performing a variation of the extended functional

$$U_{\boldsymbol{\tau}} = \frac{1}{2} \int_{\Omega} \left(\mathbf{E}^T \boldsymbol{\Sigma} - (\boldsymbol{\tau} - \boldsymbol{\lambda})^T (\mathbf{L} - \mathbf{L}_0)^{-1} (\boldsymbol{\tau} - \boldsymbol{\lambda}) \right. \\ \left. + 2 \boldsymbol{\tau}^T \mathbf{E} + \boldsymbol{\varepsilon}'^T \boldsymbol{\tau} + \boldsymbol{\lambda}^T \mathbf{L}^{-1} \boldsymbol{\lambda} \right) d\Omega. \quad (20)$$

Setting

$$\delta U_{\boldsymbol{\tau}} = -\frac{1}{2} \int_{\Omega} \left\{ 2 \delta \boldsymbol{\tau}^T \left[(\mathbf{L} - \mathbf{L}_0)^{-1} (\boldsymbol{\tau} - \boldsymbol{\lambda}) - \boldsymbol{\varepsilon} \right] + \delta \boldsymbol{\tau}^T \boldsymbol{\varepsilon}' - \delta \boldsymbol{\varepsilon}'^T \boldsymbol{\tau} \right\} d\Omega = 0, \quad (21)$$

we find that Eq. (14) is one of the stationarity conditions of $U_{\boldsymbol{\tau}}$, while the second condition, Eq. (13), follows after recasting the remaining terms in the brackets. Finally,

it can be proven that the stationary value $U_{\boldsymbol{\tau}}^S$ of the potential $U_{\boldsymbol{\tau}}$ equals the actual potential energy stored in the anisotropic and heterogeneous body

$$U_{\boldsymbol{\tau}}^S = \frac{1}{2} \int (\boldsymbol{\varepsilon} - \boldsymbol{\mu})^T \mathbf{L} (\boldsymbol{\varepsilon} - \boldsymbol{\mu}) d\Omega, \quad (22)$$

where

$$\boldsymbol{\mu} = -\mathbf{L}^{-1} \boldsymbol{\lambda}, \quad (23)$$

is the vector of eigenstrains (stress-free strains). The function $U_{\boldsymbol{\tau}}$ attains its maximum ($\delta^2 U_{\boldsymbol{\tau}} < 0$) if $(\mathbf{L} - \mathbf{L}_0)$ positive definite and its minimum if $(\mathbf{L} - \mathbf{L}_0)$ is negative definite for all $\mathbf{x} \in \Omega$.

3.2 Response of random composites

Consider the H-S functional, Eq. (20), for a given sample α . The fluctuation part of the local strain $\boldsymbol{\varepsilon}(\mathbf{x})$ reads

$$\boldsymbol{\varepsilon}'(\mathbf{x}, \alpha) = \boldsymbol{\varepsilon}(\mathbf{x}, \alpha) - \mathbf{E} = \int_{\Omega} \boldsymbol{\varepsilon}_0^*(\mathbf{x} - \mathbf{x}') (\boldsymbol{\tau}(\mathbf{x}') - \langle \boldsymbol{\tau} \rangle(\alpha)) d\Omega(\mathbf{x}'), \quad (24)$$

where the specific form of $\boldsymbol{\varepsilon}_0^*$ can be found in [9]. $\langle \boldsymbol{\tau} \rangle$ represents the mean or volume average of $\boldsymbol{\tau}(\mathbf{x})$. Subscript 0 is used to identify this operator with the homogeneous reference medium. Eq. (24) then allows to rewrite Eq. (20) as

$$\begin{aligned} U_{\boldsymbol{\tau}}(\alpha) &= \frac{1}{2} \int_{\Omega} (\mathbf{E}^T \boldsymbol{\Sigma} - (\boldsymbol{\tau}(\mathbf{x}, \alpha) - \boldsymbol{\lambda}(\mathbf{x}, \alpha))^T (\mathbf{L}(\mathbf{x}, \alpha) - \mathbf{L}_0)^{-1} (\boldsymbol{\tau}(\mathbf{x}, \alpha) - \boldsymbol{\lambda}(\mathbf{x}, \alpha)) \\ &+ 2\boldsymbol{\tau}^T(\mathbf{x}, \alpha) \mathbf{E} + \boldsymbol{\tau}^T(\mathbf{x}, \alpha) \int_{\Omega} \boldsymbol{\varepsilon}_0^*(\mathbf{x} - \mathbf{x}') (\boldsymbol{\tau}(\mathbf{x}', \alpha) - \langle \boldsymbol{\tau} \rangle(\alpha)) d\Omega(\mathbf{x}') \\ &+ \boldsymbol{\lambda}^T(\mathbf{x}, \alpha) \mathbf{L}^{-1}(\mathbf{x}, \alpha) \boldsymbol{\lambda}(\mathbf{x}, \alpha)) d\Omega(\mathbf{x}). \end{aligned} \quad (25)$$

Details are given in [9]. If each phase r of a randomly arranged composite is homogeneous with moduli $\mathbf{L}_r, r = 1, \dots, n$, then the material stiffness matrix in the sample α can be expressed as [3],

$$\mathbf{L}(\mathbf{x}, \alpha) = \sum_{r=1}^n \mathbf{L}_r \chi_r(\mathbf{x}, \alpha). \quad (26)$$

and the ensemble average of \mathbf{L} is

$$\overline{\mathbf{L}(\mathbf{x})} = \sum_{r=1}^n \mathbf{L}_r S_r(\mathbf{x}). \quad (27)$$

Similarly, the trial field for $\boldsymbol{\tau}$ and eigenstress $\boldsymbol{\lambda}$ at any point \mathbf{x} located in the sample α are provided by

$$\boldsymbol{\tau}(\mathbf{x}, \alpha) = \sum_{r=1}^n \boldsymbol{\tau}_r(\mathbf{x}) \chi_r(\mathbf{x}, \alpha), \quad \boldsymbol{\lambda}(\mathbf{x}, \alpha) = \sum_{r=1}^n \boldsymbol{\lambda}_r(\mathbf{x}) \chi_r(\mathbf{x}, \alpha), \quad (28)$$

with the respective ensemble averages written as

$$\overline{\boldsymbol{\tau}(\mathbf{x})} = \sum_{r=1}^n \boldsymbol{\tau}_r(\mathbf{x}) S_r(\mathbf{x}), \quad \overline{\boldsymbol{\lambda}(\mathbf{x})} = \sum_{r=1}^n \boldsymbol{\lambda}_r(\mathbf{x}) S_r(\mathbf{x}). \quad (29)$$

To facilitate the solution of the present problem the material is assumed to be ergodic and statistically homogeneous. Therefore,

$$\overline{\mathbf{L}} = \sum_{r=1}^n \mathbf{L}_r c_r, \quad \overline{\boldsymbol{\tau}(\mathbf{x})} = \sum_{r=1}^n \boldsymbol{\tau}_r(\mathbf{x}) c_r, \quad \overline{\boldsymbol{\lambda}(\mathbf{x})} = \sum_{r=1}^n \boldsymbol{\lambda}_r(\mathbf{x}) c_r. \quad (30)$$

Substituting Eqs. (28) and (30) into Eq (25) yields the extended averaged form of the Hashin-Shtrikman principle

$$\begin{aligned} \overline{U_{\boldsymbol{\tau}}} &= \frac{1}{2} \int_{\Omega} \left(\mathbf{E}^T \boldsymbol{\Sigma} + \sum_r c_r \boldsymbol{\lambda}_r^T(\mathbf{x}) \mathbf{L}_r \boldsymbol{\lambda}_r(\mathbf{x}) \right) d\Omega(\mathbf{x}) \\ &- \frac{1}{2} \sum_r \int_{\Omega} \left(c_r (\boldsymbol{\tau}_r(\mathbf{x}) - \boldsymbol{\lambda}_r(\mathbf{x}))^T (\mathbf{L}_r - \mathbf{L}_0)^{-1} (\boldsymbol{\tau}_r(\mathbf{x}) - \boldsymbol{\lambda}_r(\mathbf{x})) - 2c_r \boldsymbol{\tau}_r^T(\mathbf{x}) \mathbf{E} \right) d\Omega(\mathbf{x}) \\ &+ \frac{1}{2} \sum_r \sum_s \int_{\Omega} \boldsymbol{\tau}_r(\mathbf{x})^T \int_{\Omega} \boldsymbol{\epsilon}_0^*(\mathbf{x} - \mathbf{x}') [S_{rs}(\mathbf{x} - \mathbf{x}') \boldsymbol{\tau}_s(\mathbf{x}') - c_r \langle \boldsymbol{\tau} \rangle] d\Omega(\mathbf{x}') d\Omega(\mathbf{x}). \end{aligned} \quad (31)$$

Then, assuming a piecewise uniform variation of eigenstress vector $\boldsymbol{\lambda}$ and polarization stress $\boldsymbol{\tau}$ ($\boldsymbol{\lambda}_r(\mathbf{x}) = \boldsymbol{\lambda}_r, \boldsymbol{\tau}_r(\mathbf{x}) = \boldsymbol{\tau}_r$), setting (recall ergodicity assumption)

$$\langle \boldsymbol{\tau} \rangle(\alpha) = \langle \boldsymbol{\tau} \rangle = \sum_{r=1}^n \boldsymbol{\tau}_r c_r, \quad (32)$$

and then performing variation with respect to $\boldsymbol{\tau}_r$ provides the extended form of the stationarity condition

$$(\mathbf{L}_r - \mathbf{L}_0)^{-1} \boldsymbol{\tau}_r c_r - \sum_{s=1}^n \mathbf{A}_{rs} \boldsymbol{\tau}_s = c_r \mathbf{E} + (\mathbf{L}_r - \mathbf{L}_0)^{-1} c_r \boldsymbol{\lambda}_r, \quad r = 1, 2, \dots, n, \quad (33)$$

where the microstructure-dependent matrices \mathbf{A}_{rs} are independent of \mathbf{x} and are provided by

$$\begin{aligned} \mathbf{A}_{rs} &= \int_{\Omega} \boldsymbol{\epsilon}_0^*(\mathbf{x} - \mathbf{x}') [S_{rs}(\mathbf{x} - \mathbf{x}') - c_r c_s] d\Omega(\mathbf{x}') \\ &= \int_{\Omega} \boldsymbol{\epsilon}_0^*(\mathbf{x} - \mathbf{x}') S'_{rs}(\mathbf{x} - \mathbf{x}') d\Omega(\mathbf{x}') = \int_{\Omega} \boldsymbol{\epsilon}_0^*(\mathbf{x}) S'_{rs}(\mathbf{x}) d\Omega(\mathbf{x}), \end{aligned} \quad (34)$$

where S'_{rs} denotes the fluctuating part of S_{rs} under the no-long range orders hypothesis. The preceding formula can be further rewritten as

$$\begin{aligned}\mathbf{A}_{rs} &= \int_{\Omega} \boldsymbol{\varepsilon}_0^*(\mathbf{x}) S'_{rs}(\mathbf{x}) d\Omega(\mathbf{x}) \\ &= \left[\int_{\Omega} \boldsymbol{\varepsilon}_0^*(\mathbf{x}) S'_{rs}(\mathbf{x}) e^{i\mathbf{x} \cdot \boldsymbol{\xi}} d\Omega(\mathbf{x}) \right]_{\boldsymbol{\xi}=\mathbf{0}} = F[\boldsymbol{\varepsilon}_0^*(\mathbf{x}) S'_{rs}(\mathbf{x})]_{\boldsymbol{\xi}=\mathbf{0}},\end{aligned}\quad (35)$$

where the operator F represents the Fourier transform. The property of F provides

$$\mathbf{A}_{rs} = \frac{1}{(2\boldsymbol{\pi})^d} \left[\int_{\Omega} \tilde{\boldsymbol{\varepsilon}}_0^*(\boldsymbol{\xi} - \boldsymbol{\xi}') \tilde{S}'_{rs}(\boldsymbol{\xi}') d\Omega(\boldsymbol{\xi}') \right]_{\boldsymbol{\xi}=\mathbf{0}} = \frac{1}{(2\boldsymbol{\pi})^d} \int_{\Omega} \tilde{\boldsymbol{\varepsilon}}_0^*(-\boldsymbol{\xi}') \tilde{S}'_{rs}(\boldsymbol{\xi}') d\Omega(\boldsymbol{\xi}'). \quad (36)$$

Since $\tilde{\boldsymbol{\varepsilon}}_0^*(-\boldsymbol{\xi}) = \tilde{\boldsymbol{\varepsilon}}_0^*(\boldsymbol{\xi})$ we finally arrive at

$$\mathbf{A}_{rs} = \frac{1}{(2\boldsymbol{\pi})^d} \int_{\Omega} \tilde{\boldsymbol{\varepsilon}}_0^*(\boldsymbol{\xi}') \tilde{S}'_{rs}(\boldsymbol{\xi}') d\Omega(\boldsymbol{\xi}'). \quad (37)$$

Note that Fourier's transform $\tilde{\boldsymbol{\varepsilon}}_0^*$ can be obtained for any homogeneous anisotropic reference media (see [3]), which is not generally possible for function $\boldsymbol{\varepsilon}_0^*$ itself. Therefore, once we are able to compute the values of \tilde{S}'_{rs} we may evaluate integral (37) by an appropriate numerical procedure. Finally, having determined the value of \mathbf{A}_{rs} , the solution of system (33) can be formally written in the form

$$\boldsymbol{\tau}_r = \sum_{s=1}^n \mathbf{T}_{rs} c_s \left[\mathbf{E} + (\mathbf{L}_s - \mathbf{L}_0)^{-1} \boldsymbol{\lambda}_s \right], \quad (38)$$

from which

$$\bar{\boldsymbol{\tau}} = \sum_{r=1}^n \sum_{s=1}^n c_r \mathbf{T}_{rs} c_s \left[\mathbf{E} + (\mathbf{L}_s - \mathbf{L}_0)^{-1} \boldsymbol{\lambda}_s \right]. \quad (39)$$

Once the matrices \mathbf{T}_{rs} are known, the overall constitutive law yields

$$\bar{\boldsymbol{\sigma}} = \hat{\mathbf{L}} \mathbf{E} + \bar{\boldsymbol{\lambda}}, \quad (40)$$

where

$$\hat{\mathbf{L}} = \mathbf{L}_0 + \sum_{r=1}^n \sum_{s=1}^n c_r \mathbf{T}_{rs} c_s, \quad (41)$$

$$\bar{\boldsymbol{\lambda}} = \sum_{r=1}^n \sum_{s=1}^n c_r \mathbf{T}_{rs} c_s (\mathbf{L}_s - \mathbf{L}_0)^{-1} \boldsymbol{\lambda}_s. \quad (42)$$

4 Effective properties by periodic unit cell approach

This section presents another approach to the analysis of random composites, which relies on a *periodic unit cell*. This concept is very convenient from the point of view of numerical analysis, as it allows to simulate wide range of inelastic behavior of composites (see eg. [6] and references therein). The crucial point now becomes to incorporate the random character of a microstructure into this approach. Here, we offer a simple procedure based on aforementioned microstructural statistics.

4.1 Formulation of Periodic Unit Cell

In our previous work [12] we suggested that both the two-point probability function and the second-order intensity function can be exploited to generate the desired periodic unit cell (PUC). Such a PUC should possess similar statistical properties as the original material. We argue that if the PUC has a statistically similar spatial distribution of fibers as the real microstructure it will also possess similar thermomechanical properties. The PUC is constructed here by matching the second-order intensity functions of the real microstructure and the unit cell

$$F(x^N, H_1, H_2) = \sum_{i=1}^{N_m} \left(\frac{\bar{K}(r_i) - K(r_i)}{\pi r_i^2} \right)^2, \quad (43)$$

where $\bar{K}(r_i)$ represents the second order intensity function of the original microstructure, $K(r_i)$ corresponds to the PUC and N_m is the number of matching points. Vector $x = \{x^1, y^1, \dots, x^N, y^N\}$ stands for the configuration of particle centers of the periodic unit cell; x^i and y^i correspond to x and y coordinates of the i -th particle. The augmented simulated annealing method can be used to minimize the objective function Eq. (43). Details of the algorithm can be found in [5]. Two representatives of the periodic unit cell constructed for the graphite/epoxy material system are displayed in Fig. 3.

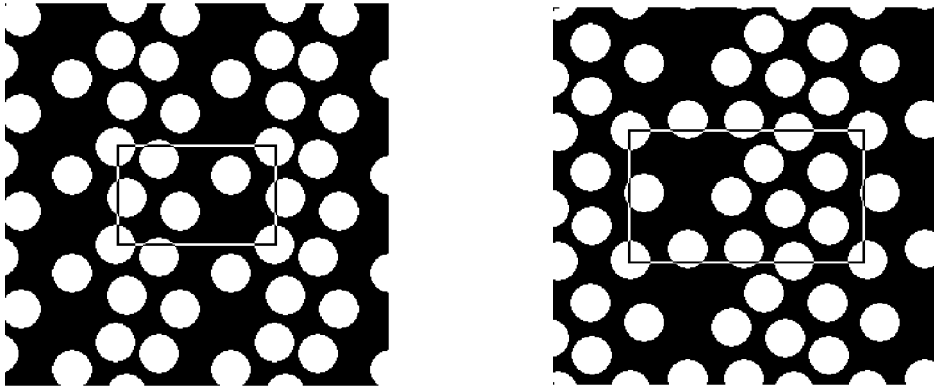


Figure 3: Periodic unit cells: (a) 5-fibres PUC, (b) 10-fibres PUC

4.2 Thermomechanical problem

We now recall the thermomechanical analysis of a representative volume element (RVE) having well defined geometry and boundary conditions. In particular we consider a periodic representative volume defined in terms of a statistically equivalent unit cell (UC) derived in the preceding part.

Suppose that the UC is subjected to boundary displacements \mathbf{u} and uniform change of temperature $\Delta\theta$ resulting in a uniform strain \mathbf{E} throughout the UC. The local constitutive equation is then written in the form

$$\boldsymbol{\sigma}(\mathbf{x}) = \mathbf{L}(\mathbf{x})[\boldsymbol{\varepsilon}(\mathbf{u}(\mathbf{x})) - \boldsymbol{\varepsilon}_0(\mathbf{x})], \quad (44)$$

where $\boldsymbol{\varepsilon}_0(\mathbf{x}) = \mathbf{m}(\mathbf{x})\Delta\theta$ represents the initial thermal strain or eigenstrain; vector $\mathbf{m}(\mathbf{x})$ lists the coefficients of thermal expansion for the material point \mathbf{x} . In view of the periodic boundary conditions imposed on the unit cell the strain and displacement fields in the UC admit the following decomposition

$$\mathbf{u}(\mathbf{x}) = \mathbf{E} \cdot \mathbf{x} + \mathbf{u}^*(\mathbf{x}), \quad (45)$$

$$\boldsymbol{\varepsilon}(\mathbf{x}) = \mathbf{E} + \boldsymbol{\varepsilon}^*(\mathbf{x}). \quad (46)$$

The periodicity of \mathbf{u}^* implies that the average of $\boldsymbol{\varepsilon}^*$ in the unit cell vanishes. Hence

$$\langle \boldsymbol{\varepsilon}(\mathbf{x}) \rangle = \mathbf{E} + \langle \boldsymbol{\varepsilon}^*(\mathbf{x}) \rangle, \quad \langle \boldsymbol{\varepsilon}^*(\mathbf{x}) \rangle = \frac{1}{\Omega} \int_{\Omega} \boldsymbol{\varepsilon}^*(\mathbf{x}) d\mathbf{x} = \mathbf{0}. \quad (47)$$

Next, assume a virtual displacement $\delta\mathbf{u} = \delta\mathbf{E} \cdot \mathbf{x} + \delta\mathbf{u}^*$, with $\delta\mathbf{u}^*$ being periodic. Then

$$\langle \delta\boldsymbol{\varepsilon}^T \boldsymbol{\sigma} \rangle = \delta\mathbf{E}^T \boldsymbol{\Sigma}, \quad \boldsymbol{\Sigma} = \langle \boldsymbol{\sigma} \rangle. \quad (48)$$

Eq. (48), also known as the Hill lemma, implies that the average microscopic internal work is precisely the macroscopic virtual work.

It is often convenient to impose surface tractions compatible with the macroscopic uniform state of stress $\boldsymbol{\Sigma}$. Such a loading condition is more general but leaves us with unknown overall strain \mathbf{E} and periodic displacement field \mathbf{u}^* to be determined. Substituting the microscopic constitutive equation (44) into Hill's lemma Eq. (48) gives

$$\langle \delta\boldsymbol{\varepsilon}^{*T} \boldsymbol{\sigma} \rangle = \langle \delta\boldsymbol{\varepsilon}^{*T} \mathbf{L}(\boldsymbol{\varepsilon}(\mathbf{u}) - \boldsymbol{\varepsilon}_0) \rangle = \delta\mathbf{E}^T \boldsymbol{\Sigma}, \quad (49)$$

and consequently with the help of Eq. (46) we find

$$\delta\mathbf{E}^T \langle \mathbf{L}(\mathbf{E} + \boldsymbol{\varepsilon}^* - \boldsymbol{\varepsilon}_0) \rangle + \langle \delta\boldsymbol{\varepsilon}^{*T} \mathbf{L}\mathbf{E} \rangle + \langle \delta\boldsymbol{\varepsilon}^{*T} \mathbf{L}(\boldsymbol{\varepsilon}^* - \boldsymbol{\varepsilon}_0) \rangle = \delta\mathbf{E}^T \boldsymbol{\Sigma}. \quad (50)$$

Since $\delta\mathbf{E}$ and $\delta\boldsymbol{\varepsilon}^*$ are independent, the preceding equation can be split into two equalities

$$\begin{aligned}\delta \mathbf{E}^T \boldsymbol{\Sigma} &= \delta \mathbf{E}^T \left[\langle \mathbf{L} \rangle \mathbf{E} + \mathbf{L} \langle \boldsymbol{\varepsilon}^* - \boldsymbol{\varepsilon}_0 \rangle \right], \\ \mathbf{0} &= \langle \delta \boldsymbol{\varepsilon}^{*T} \mathbf{L} \rangle \mathbf{E} + \langle \delta \boldsymbol{\varepsilon}^{*T} \mathbf{L} (\boldsymbol{\varepsilon}^* - \boldsymbol{\varepsilon}_0) \rangle.\end{aligned}\quad (51)$$

In the FE approach the matrix \mathbf{B} , relating strains and displacements in the form $\boldsymbol{\varepsilon}^* = \mathbf{B}\mathbf{u}^*$ and consequently, $\delta \boldsymbol{\varepsilon}^* = \mathbf{B}\delta \mathbf{u}^*$, is to be applied to Eq. (51) to get the linear associated system

$$\begin{bmatrix} \frac{1}{\Omega} \int_{\Omega} \mathbf{L} d\Omega & \frac{1}{\Omega} \int_{\Omega} \mathbf{L} \mathbf{B} d\Omega \\ \frac{1}{\Omega} \int_{\Omega} \mathbf{B}^T \mathbf{L} d\Omega & \frac{1}{\Omega} \int_{\Omega} \mathbf{B}^T \mathbf{L} \mathbf{B} d\Omega \end{bmatrix} \begin{Bmatrix} \mathbf{E} \\ \mathbf{u}^* \end{Bmatrix} = \begin{Bmatrix} \boldsymbol{\Sigma} + \frac{1}{\Omega} \int_{\Omega} \mathbf{L} \boldsymbol{\varepsilon}_0 d\Omega \\ \frac{1}{\Omega} \int_{\Omega} \mathbf{B}^T \mathbf{L} \mathbf{B} d\Omega \end{Bmatrix}.\quad (52)$$

When excluding the thermal effects the above equation can be used to derive the coefficients of the effective compliance matrix \mathbf{M} as volume averages of the local fields from the solution of four successive elasticity problems. To that end, the periodic unit cell is loaded, in turn, by each of the components of $\boldsymbol{\Sigma}$, while the other remaining components vanish. The volume strain averages normalized with respect to $\boldsymbol{\Sigma}$ then furnish individual columns of \mathbf{M} . However, when the UC is loaded by uniform temperature change equal to unity, the components of the overall average strain then comply with the effective coefficients of thermal expansion \mathbf{m} .

4.3 Macroscopic constitutive law by averaging

In this section we examine connections between the thermal and mechanical properties of composite materials. In particular, we rederive the macroscopic constitutive law of composites subjected to thermomechanical loading by means of standard averaging. We start with the local constitutive law written as

$$\boldsymbol{\varepsilon}(\mathbf{x}) = \mathbf{M}(\mathbf{x})\boldsymbol{\sigma}(\mathbf{x}) + \Delta\theta \mathbf{m}(\mathbf{x}).\quad (53)$$

Next, recall the strain volume average in the form

$$\begin{aligned}\langle \boldsymbol{\varepsilon}(\mathbf{x}) \rangle &= \frac{1}{\Omega} \int_{\Omega} [\mathbf{M}(\mathbf{x})\boldsymbol{\sigma}(\mathbf{x}) + \Delta\theta \mathbf{m}(\mathbf{x})] d\Omega \\ &= \mathbf{E} + \langle \boldsymbol{\varepsilon}^*(\mathbf{x}) \rangle, \quad \langle \boldsymbol{\varepsilon}^*(\mathbf{x}) \rangle = 0,\end{aligned}\quad (54)$$

which directly provides the macroscopic constitutive law

$$\frac{1}{\Omega} \int_{\Omega} [\mathbf{M}(\mathbf{x})\boldsymbol{\sigma}(\mathbf{x}) + \Delta\theta \mathbf{m}(\mathbf{x})] d\Omega = \mathbf{M}\boldsymbol{\Sigma} + \Delta\theta \mathbf{m}.\quad (55)$$

Introducing the mechanical and thermal stress influence functions $\mathbf{B}(\mathbf{x})$ and $\mathbf{b}(\mathbf{x})$, respectively, such that

$$\boldsymbol{\sigma}(\mathbf{x}) = \mathbf{B}(\mathbf{x})\boldsymbol{\Sigma} + \mathbf{b}(\mathbf{x})\Delta\theta,\quad (56)$$

we find

$$\langle \boldsymbol{\sigma}(\mathbf{x}) \rangle = \int_{\Omega} \mathbf{M}(\mathbf{x}) \mathbf{B}(\mathbf{x}) d\Omega \boldsymbol{\Sigma} + \int_{\Omega} \mathbf{M}(\mathbf{x}) (\mathbf{b}(\mathbf{x}) + \mathbf{m}(\mathbf{x})) d\Omega \Delta\theta. \quad (57)$$

When assuming piecewise uniform variation of phase thermal and elastic properties, Eq. (57) readily provides the macroscopic compliance matrix \mathbf{M} and the macroscopic thermal strain vector \mathbf{m} as

$$\mathbf{M} = \sum_r c_r \mathbf{M}_r \mathbf{B}_r, \quad \mathbf{m} = \sum_r c_r (\mathbf{M}_r \mathbf{b}_r + \mathbf{m}_r). \quad (58)$$

When admitting only thermal effects, $\boldsymbol{\Sigma} = \mathbf{0}$, we get

$$\langle \boldsymbol{\sigma}(\mathbf{x}) \rangle = \sum_r \frac{\Omega_r}{\Omega} \int_{\Omega} \mathbf{b}(\mathbf{x}) d\Omega = \sum_r c_r \mathbf{b}_r = \mathbf{0}. \quad (59)$$

It is also useful to recall the familiar Levin formula given by

$$\mathbf{m} = \sum_r c_r \mathbf{B}_r^T \mathbf{m}_r. \quad (60)$$

When setting $\Delta\theta = 0$ the system (52) can be used to extract the phase concentration factor tensor \mathbf{B}_r . The phase thermal stress concentration factor \mathbf{b}_r follows again from Eq. (52) when setting $\boldsymbol{\Sigma} = \mathbf{0}$, $\Delta\theta = 1$, as phase volume average of the local stress found in the phase r . Thus both Eqs. (52) and (58) can be exploit to obtain the effective compliances and coefficients of thermal expansion listed in vector \mathbf{m} .

5 Results

This section summarizes numerical results derived from both approaches for the graphite-epoxy composite system displayed in Figure 1. The material properties are stored in Table 1. The analysis was carried out under the generalized plane strain conditions.

Table 1: Material properties of T30/Epoxy system

phase	E_A [GPa]	E_T [GPa]	G_T [GPa]	ν_A	α_A [K ⁻¹]	α_T [K ⁻¹]
-------	----------------	----------------	----------------	---------	----------------------------------	----------------------------------

fiber	386	7.6	2.6	0.41	-1.2×10^{-6}	7×10^{-6}
matrix	5.5	5.5	1.96	0.40	2.4×10^{-5}	2.4×10^{-5}

Tables 2 and 3 list effective elastic stiffnesses and coefficients of thermal expansion found from the Hashin-Shtrikman variational principle. The Fourier transform of S'_{rs} was first obtained by applying the discrete Fourier transform (DFT) to digitized image of Fig. 1. The integral formula (37) was then evaluated to get the desired microstructure-dependent matrices \mathbf{A}_{rs} . When incorporating these matrices into Eqs. (41) and (42) we get the overall effective stiffness matrix $\hat{\mathbf{L}}$ and the overall thermal stresses $\bar{\boldsymbol{\lambda}} = -\hat{\mathbf{L}}\mathbf{m}$.

In addition, the effective moduli together with thermal expansion coefficients derived for selected periodic unit cells are stored in Tables 4 and 5. Clearly, the Finite Element solutions fall within individual bounds. Moreover, slight anisotropy possessed by the present microstructure can be captured by this approach. Finally, Table 6 shows that the values of effective coefficients of thermal expansion obtained using relations (52), (58) and (60) are identical.

When compared to the unit cell approach the method based on the Hashin-Shtrikman variational principle is much faster and thus preferable when evaluating the macroscopic elastic response of real composites. Not the same might be true when inelastic deformations are decisive. But this has yet to be confirmed.

Table 2: HS principle approach : Effective elastic stiffnesses [GPa]

Bitmap resolution	L_{11}			L_{22}			L_{33}		
	LB	FEM	UB	LB	FEM	UB	LB	FEM	UB
122 X 84	10.733	10.762	10.770	10.713	10.725	10.746	2.211	2.215	2.218
244 X 179	10.740	10.762	10.777	10.720	10.725	10.752	2.209	2.215	2.216
488 X 358	10.730	10.762	10.763	10.721	10.725	10.754	2.209	2.215	2.216
976 X 716	10.730	10.762	10.763	10.721	10.725	10.764	2.209	2.215	2.216

Table 3: HS principle approach : Effective coefficients of thermal expansions [K^{-1}]

Bitmap resolution	$\alpha_x \times 10^5$			$\alpha_y \times 10^5$			$\alpha_z \times 10^5$			c_f
	LB	FEM	UB	LB	FEM	UB	LB	FEM	UB	
122 X 84	2.248	2.269	2.278	2.230	2.248	2.253	-7.488	-7.463	-7.504	0.438
244 X 179	2.256	2.269	2.285	2.236	2.248	2.259	-7.455	-7.463	-7.471	0.436
488 X 358	2.256	2.269	2.287	2.237	2.248	2.260	-7.455	-7.463	-7.471	0.436
976 X 716	2.256	2.269	2.287	2.237	2.248	2.260	-7.455	-7.463	-7.471	0.436

Table 4: PUC approach: Effective elastic stiffness [GPa]

Unit cell	L_{11}	L_{22}	L_{33}	L_{44}	c_f
Original	10.76	10.73	2.215	177.2	0.44

2 fibres PUC	10.78	10.75	2.202	177.2	0.44
5 fibres PUC	10.76	10.73	2.215	177.2	0.44
10 fibres PUC	10.76	10.73	2.215	177.2	0.44
Hexagonal array	10.74	10.74	2.213	177.3	0.44

Table 5: PUC approach: Effective coefficients of thermal expansion [K^{-1}]

Unit cell	$\alpha_x \times 10^5$	$\alpha_y \times 10^5$	$\alpha_z \times 10^5$
Original	2.290	2.268	-7.319
2 fibres PUC	2.293	2.267	-7.318
5 fibres PUC	2.285	2.267	-7.319
10 fibres PUC	2.289	2.267	-7.319
Hexagonal array	2.285	2.285	-7.279

Table 6: Comparison of relations (52),(58) and (60) for 5-fiber PUC [K^{-1}]

Relation	$\alpha_x \times 10^5$	$\alpha_y \times 10^5$	$\alpha_z \times 10^5$
Equation 52	2.285	2.267	-7.319
Equation 58	2.285	2.267	-7.319
Equation 60	2.285	2.267	-7.319

6 Conclusions

Effective thermoelastic properties were found for a fibrous graphite-epoxy composite system with fibers randomly distributed within a transverse plane section of the composite aggregate. Two reliable and efficient approaches were introduced in the present work. Although different at their theoretical formulation both approaches are closely tight to the same statistical descriptors generally used to quantify random microstructures.

The first approach discussed in Section 2 is closely related to well known effective medium theories. Here, the most widely used variational principle of Hashin and Shtrikman was reviewed and extended. A very efficient numerical procedure based on the DFT which directly exploits digitized images of real microstructures was implemented. Fourier transform approach applied when solving the resulting integral equations is rather advantageous as it allows an arbitrary choice of the reference medium so that often encountered anisotropy of individual phases creates no obstacles in the solution procedure.

The second approach is based on construction of various periodic unit cell models combined with the finite element method. The complexity of real microstructures was reflected here in more complicated unit cells having larger number of particles. The required number of particles and their arrangement was determined such that the macroscopic response of a unit cell should be identical to the behavior of a real composite. A simple and intuitive approach based on microstructural statistics was proposed to derive such periodic unit cells. An applicability of the present approach

was confirmed by evaluating effective thermoelastic properties of the selected composite system from both the small period unit cells (five to ten fibers unit cells) and considerably larger unit cells having of two orders of magnitude more particles (three to five hundred fibers). The supplemented numerical examples showed that the PUC with a small number of reinforcement was able to capture the overall behavior of random composites with a considerable level of confidence.

Acknowledgments

Financial support was provided by the Ministry of Education, project No. MSM 210000003

References

- [1] Beran, M.J. (1968) Statistical continuum theories, Interscience publishers, a division of John Wiley and Sons, New York.
- [2] Bittnar, Z. and Šejnoha, J. (1996) Numerical methods in structural mechanics, ASCE Press.
- [3] Drugan, W.J. and Willis, J.R. (1996) A micromechanics-based nonlocal constitutive equation and estimates of representative volume element size for elastic composites, *J. Mech. Phys. Solids*, **44** (4), 497-524.
- [4] Dvorak, G.J. and Benveniste, Y. (1992) On transformation strains and uniform fields in multiphase elastic media, *Proc. R. Soc. Lond. A* **437**, 291-310.
- [5] Matouš, K., Lepš, M., Zeman, J. and Šejnoha, M. (2000) Applying genetic algorithms to selected topics commonly encountered in engineering practice, in *Comput. Methods Appl. Mech. Engrg.*, **190**, 1629-1650
- [6] Michel, J.C., Moulinec, H., Suquet, P. (1999) Effective properties of composite materials with periodic microstructure: a computational approach, *Comput. Methods Appl. Mech. Engrg.*, **172**, 109-143.
- [7] Milton, G. W. (1982) Bounds on the elastic and transport properties of two-component composites, *J. Mech. Phys. Solids*, **30** (3), 177-191
- [8] Ripley, B. (1977) Modelling spatial patterns, *Journal of the Royal Statistical Society B*, **39** (2), 172-192.
- [9] Šejnoha, M. and Zeman, J. (2000) Micromechanical analysis of random composites *In preparation*
- [10] Torquato, S. and Stell, G. (1982) Microstructure of two-phase random media. I. The n -point matrix probability functions, *Journal of Chemical Physics*, **77**(4), 2071-2077.
- [11] Torquato, S. and Stell, G. (1985) Microstructure of two-phase random media. V. The n -point matrix probability functions for impenetrable spheres, *Journal of Chemical Physics*, **82**(2), 980-987.
- [12] Zeman J. and Šejnoha M. (2001) Numerical evaluation of effective elastic properties of graphite fiber tow impregnated by polymer matrix, in *Journal of the Mechanics and Physics of Solids*, **49**(1), 69-90